IEEE Access
Multidisciplinary | Rapid Review | Open Access Journal

Received October 31, 2019, accepted November 11, 2019, date of publication November 21, 2019, date of current version January 3, 2020.

Digital Object Identifier 10.1109/ACCESS.2019.2954984

Millimeter-Wave Broadband Tunable Band-Pass Filter Based on Liquid Crystal Materials

DI JIANG[1,2], (Member, IEEE), XIAOYU LI[1], (Student Member, IEEE), ZIHAO FU[3], GUOFU WANG[4], ZHI ZHENG[1], (Member, IEEE), TIANLIANG ZHANG[3], (Member, IEEE), AND WEN-QIN WANG[1,2], (Senior Member, IEEE)

[1]School of Information and Communication Engineering, University of Electronic Science and Technology of China, Chengdu 611731, China
[2]National Key Laboratory of ATR, National University of Defense Technology, Changsha 410073, China
[3]School of Physics, University of Electronic Science and Technology of China, Chengdu 611731, China
[4]School of Electrical and Information Engineering, Guangxi University of Technology, Liuzhou 545006, China

Corresponding author: Zihao Fu (13429777184@163.com)

This work was supported in part by the National Natural Science Foundation of China under Grant 61871086 and Grant 61761009, and in part by the International Co-operation Support Plan of Sichuan Province under Grant 2018HH0155.

ABSTRACT In this paper, a wideband band-pass frequency tunable filter using liquid crystal is proposed for millimeter-wave applications, which achieves the band-pass characteristics by introducing four transmission zeros. The main filter structure is the ring resonator loaded with two quarter-wavelength open stubs using inverted microstrip structure. The ring resonator contacts directly with the liquid crystal layer to control the bias voltage to adjust the dielectric constant of the liquid crystal material. Experimental results show that the central frequency reconstruction range varies from 27.7GHz to 24.6GHz, and the corresponding relative bandwidth changes from 48.17% to 49.82%. The group delay within the pass-band is less than 0.45ns before and after the filter reconstruction, which indicates its applicability in K-band filter.

INDEX TERMS Wideband bandpass filter, tunable, liquid crystal, ring resonator.

I. INTRODUCTION

To handle the requirement of intelligent frequency reconfiguration for devices, it is important to adopt reconfigurable filters. Recently, several papers have discussed the response frequency reconfiguration of low-pass, high-pass, band-pass and band-stop filters. The purpose is to make the filter's response frequency to change in accordance with the user's needs.

Currently the main ways to realize reconfigurable radio frequency (RF) passive devices include: PIN diode-based switching devices [1]–[4], varactor tuning [5]–[7], MEMS system [8]–[10] and tunable media. Tunable medium mainly consists of liquid crystal, ferrite [11] and graphene [12]. Compared with diodes, adjustable media is suitable for high frequency band due to no parasitic effects. However, diode has shorter tuning time than the tunable medium. Although RF MEMS has good tuning performance, it is difficult and expensive to design and implement. On the other hand, compared with ferrite, because liquid crystal is an electronic control medium, it has the advantages of saved space, easy integration and low processing cost. Liquid crystal reconfigurable technology can solve high frequency nonlinearity, high loss and difficulty in designing traditional reconfigurable filters.

In this paper, we study reconfigurable RF front-end passive bandpass filter and a novel wideband bandpass center frequency tunable filter using liquid crystal for K-band applications.

The associate editor coordinating the review of this manuscript and approving it for publication was Xiaoguang "Leo" Liu.

II. THEORY OF LIQUID CRYSTAL

A. THEORY OF LIQUID CRYSTAL MICROWAVE TRANSMISSION LINE

Liquid crystal is mainly used in microwave circuit to build liquid crystal circuit. New liquid crystal transmission lines such as substrate integrated waveguide [13] and CRLH-transmission line [14] have also been proposed.

Traditional liquid crystal transmission line can be implemented by inverted microstrip, as shown in Fig. 1, which is divided into upper, middle and lower layers: The upper circuit includes RF circuit and microstrip-inverted microstrip conversion circuit. The middle layer is a liquid crystal cavity, and the required liquid crystal layer area is obtained by the

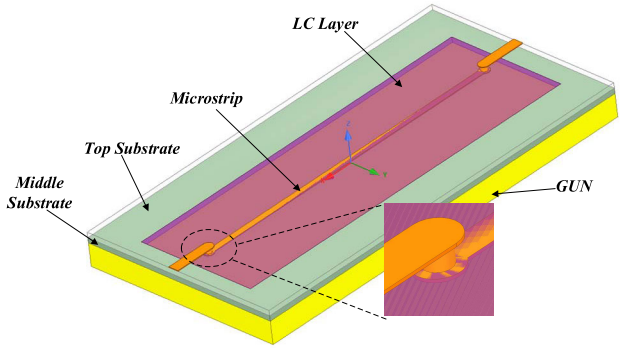

FIGURE 1. Schematic diagram of liquid crystal inverted microstrip circuit.

milling process. The thickness is the same as that of the middle layer, and the bottom is a metal ground.

When the thickness of the upper dielectric substrate is less than the strip line width, the dielectric constant of the top dielectric substrate is not considered. Similar to traditional microstrip lines, the liquid crystal inverted microstrip transmission lines propagate quasi-TEM waves. When the liquid crystal material is filled between the microstrip line and the ground, and the thickness of the inverted microstrip line is much smaller than that of the dielectric substrate, its characteristic impedance can be expressed as [15]:

$$Z_0 \propto \frac{1}{\sqrt{\varepsilon_{re}}} \tag{1}$$

Therefore, the transmission line impedance will vary with the dielectric constant of liquid crystals.

B. TUNING THEORY OF LIQUID CRYSTAL MICROSTRIP

Since liquid crystal inverted microstrip propagates quasi-TEM wave, the liquid crystal molecule distribution on the inverted microstrip lines is shown in Fig.2. As liquid crystal molecule is sensitive to low frequency signals, the influence of RF signals on liquid crystal molecules can be neglected. To deflect the liquid crystal molecule, it is necessary to introduce an additional low frequency bias signal and it is common in engineering to use 1 kHz square wave signal as the bias signal.

To ensure that the bias signal reaches the whole circuit, the liquid crystal passive devices have to be directly connected to constitute low-frequency path, and the upper signal and the bottom metal ground cannot be connected. Otherwise, it will cause a short circuit to make the upper and lower layers cannot form an electric field.

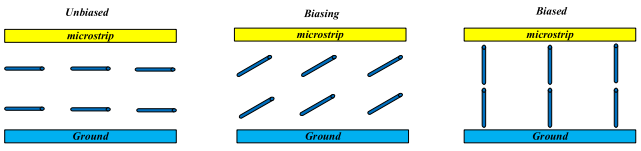

FIGURE 2. The deflection of liquid crystal molecules in an inverted microstrip.

The liquid crystal layer should be as thin as possible to ensure effective tuning for the liquid crystal. Generally, when the strip thickness is less than 0.08mm, the traditional PCB technique cannot guarantee the required accuracy, it is necessary to consider the synthesis in circuit design. Fig.3 shows the effect of different liquid crystal layer thickness on the phase shift of 100 mm inverted microstrip transmission line at 2.2GHz. When the liquid crystal layer thickness h is greater than 0.508mm, the phase shifter basically has no phase shift change. When the thickness of the liquid crystal layer is less than 0.254mm, the bias voltage can drive the liquid crystal molecule to deflect normally.

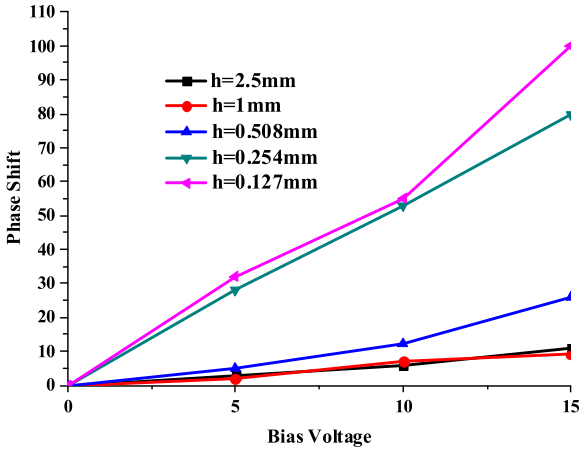

FIGURE 3. Phase shift curve of transmission line with thickness of liquid crystal layer.

III. FILTER DESIGN

AS filter is a frequency selective circuit module, by loading liquid crystal material, the filter's frequency response can be tuned, that is, the dielectric cavity perturbation in the resonator can be realized. The design difficulty of liquid crystal reconfigurable filter lies in the bias network. The traditional filter with multi-order coupling structure needs to load external bias network, which increases greatly the design difficulty. On the contrary, the filter with linear structure can only achieve relatively simple band-stop characteristics. Designing reconfigurable bandpass filters with liquid crystal materials is relatively mature. Moreover, compared with traditional PIN diode switching devices and micro-electromechanical systems, liquid crystal reconfigurable filter owns better linear tuning and simple circuit design.

A. RING RESONANCE THEORY

The ring resonator is a traditional form of filter implementation with two paths between the input port and the output port, which has dual-mode characteristics. As shown in Fig.4, the frequency response is a set of degenerate modes. When the input and output ports are located at 1, 3 or 2, 4, the resonant frequencies of the degenerate modes are the same due to symmetrical electrical length of the resonant modes and only one resonant peak, as depicted in Fig.5.

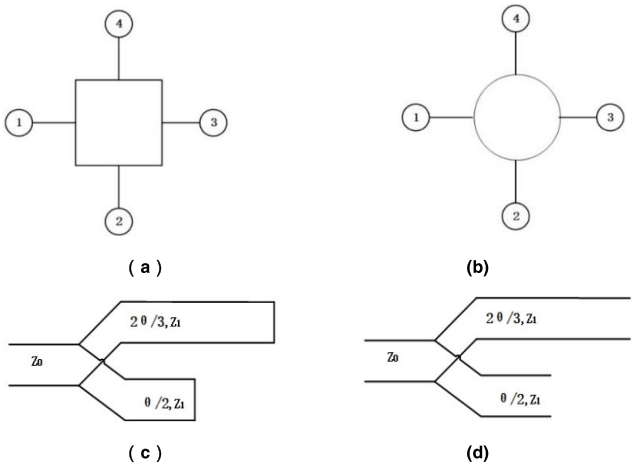

FIGURE 4. Ring resonant structure(a) square ring(b) ring shape(c) Odd-mode equivalent circuit diagram(d) Dual-mode equivalent circuit diagram.

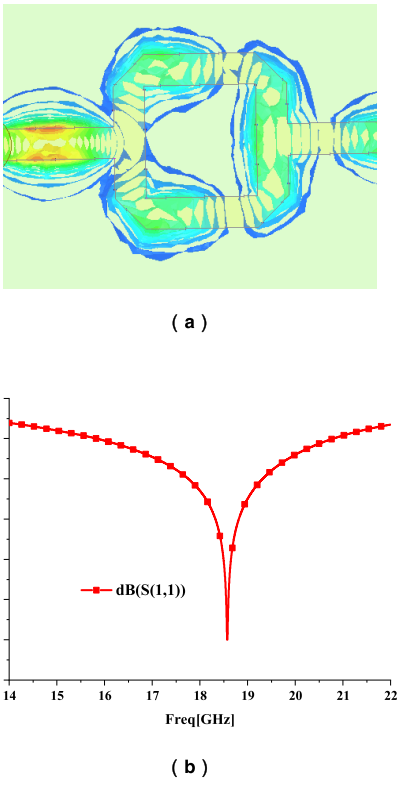

FIGURE 5. Resonant characteristics of symmetrical ports(a) Electric field distribution(b) Resonance characteristics.

Compared with the S parameter of Fig.5, the two-mode resonance is realized by separating the degenerate modes through the asymmetric distribution of two feeding ports (0°, 270°) in Fig.6 (the certain frequency is 17GHz).

B. RESEARCH ON CONSTRUCTION TECHNOLOGY OF TRANSMISSION ZERO POINT

By loading open-circuit resonant stubs, the number of resonant modes is increased, thereby the transmission zero is also increased. The equivalent circuit diagram of the square-ring resonator under the odd-mode excitation is illustrated in Fig.7.

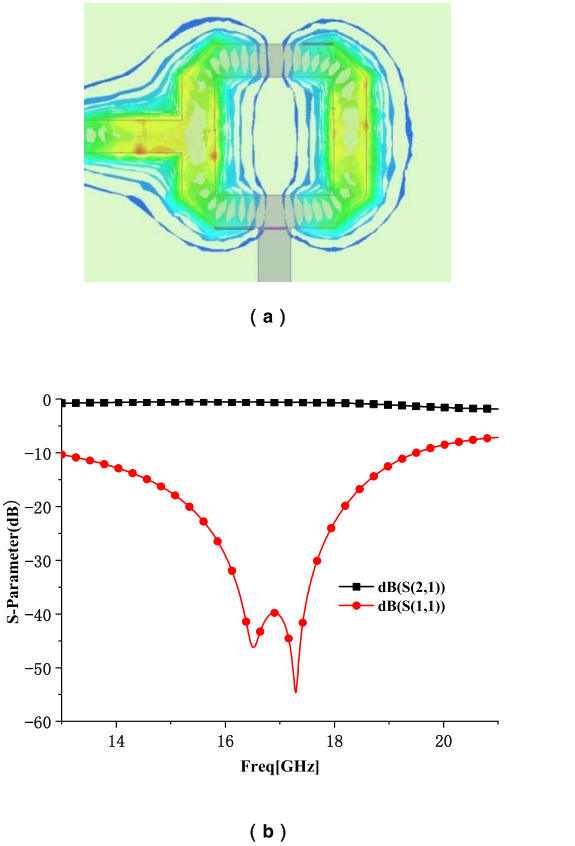

FIGURE 6. Resonance characteristics of asymmetric ports (a) Electric field distribution (b) Resonance characteristics.

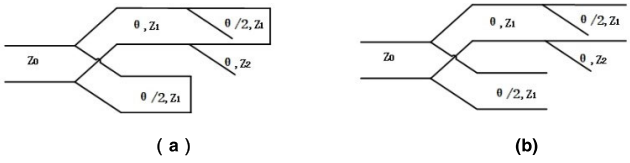

FIGURE 7. Loaded open stub equivalent circuit diagram (a) Odd Mode (b) Dual Mode.

To ensure high channel isolation frequency, an additional open-circuit stub is added at the position of Fig.8(a). Meanwhile, the resonator has four transmission zeros, four transmission zeros are located at both sides of the passband, which response frequency is

$$\tan\theta_p/2 = \pm\sqrt{\frac{Z_2}{Z_1}+1\pm\sqrt{\frac{Z_2^2}{Z_1}+2\frac{Z_1}{Z_2}}} \qquad (2)$$

where θ_p is electrical length of the open stub, Z_1 is the square ring characteristic impedance, and Z_2 is the open stub characteristic impedance. The ratio of characteristic impedance of square ring open stub is derived reversibly from Equation (2) [16]. When $Z_1 = 50\Omega$, the resonant frequency of transmission zeros is determined by Z_2. Therefore,

TABLE 1. Compared with other frequency reconfigurable filters.

	center frequency	size	number of transmissions zero	insertion loss	bandwidth	tuning range	Type of Material	publication years
[17]	20GHz	9mm×4mm	3	6dB	1GHz	2GHz	---	2010
[18]	33GHz	---	3	4.5dB	3.3GHz	2GHz	E7	2012
[13]	22GHz	6.92mm×6mm	3	6dB	600MHz	610MHz	GT5-series	2015
[19]	18.52 GHz - 20.92 GHz	12.8 mm × 6.4 mm	1	2.8 dB	--	2.9 GHz	liquid metal	2016
[20]	5.7 GHz	29.4 mm × 29.4 mm	2	1.4 dB	1.98 GHz -3.2 GHz	21.7%	---	2017
[21]	30GHz	38.3mm×48mm	3	2 -4dB	11%	700 MHz	GT3-23001	2018
[22]	60GHz	---	3	4.9 -6.2dB	1%	2.5%	GT3-23001	2019
This work	25GHz	20mm×20mm	4	5dB	13GHz	3GHz	AY71-007	

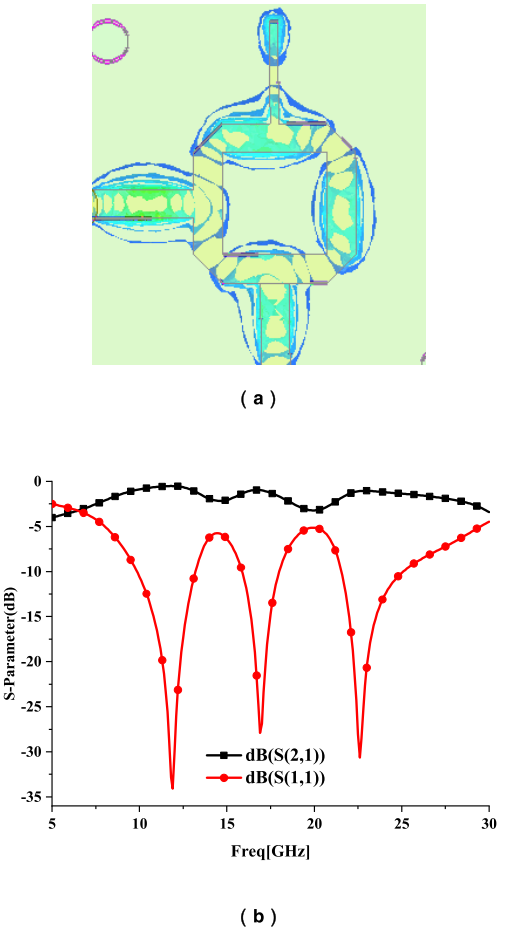

FIGURE 8. Resonance characteristics of loaded open-circuit stubs(a) Electric field distribution(b) Resonance characteristics.

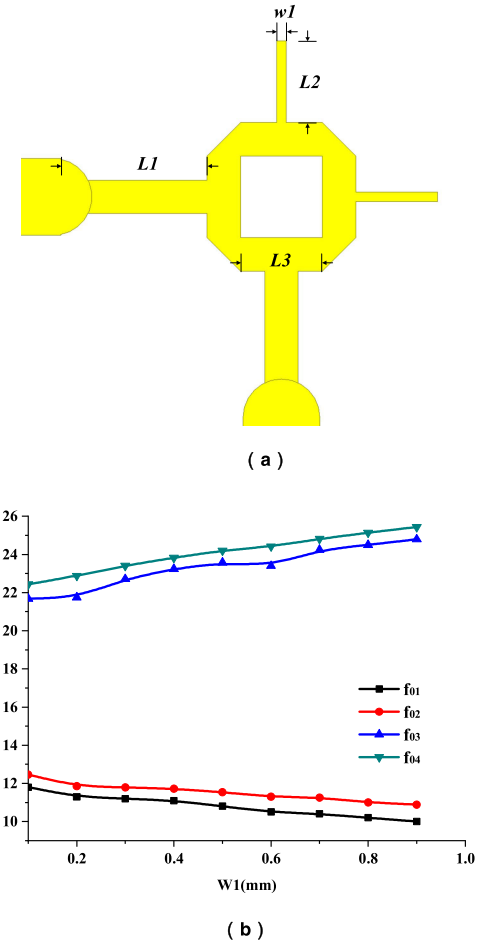

FIGURE 9. Resonance characteristics of loaded double stubs(a) Resonator layout(b) Frequency response of resonance point.

the transmission zero can be changed by controlling the open stub impedance, i.e., the stub width. Fig. 9 shows the resonant frequency variation of four transmission zeros with the open sub width "W_1".

The wideband filter is formed by adjusting the transmission zeros. When they are 11GHz, 12GHz, 21.8GHz and 23GHz, $Z_2/Z_1 = 1.66$, that is, $Z_1 = 50\Omega$, $Z_2 = 83\Omega$, and the line width is 0.2mm. Finally, the frequency response of the ring resonator simulated by CST is plotted in Fig.10.

C. DEVELOPMENT OF CENTER FREQUENCY RECONFIGURABLE BANDPASS FILTER

The inverted microstrip is divided into three parts: The upper circuit substrate as the cover plate, the middle liquid crystal layer and the bottom metal ground.

To weld joints conveniently, the upper circuit part is introduced into the lower surface of the substrate through metallized with vias. The square ring resonant structure is

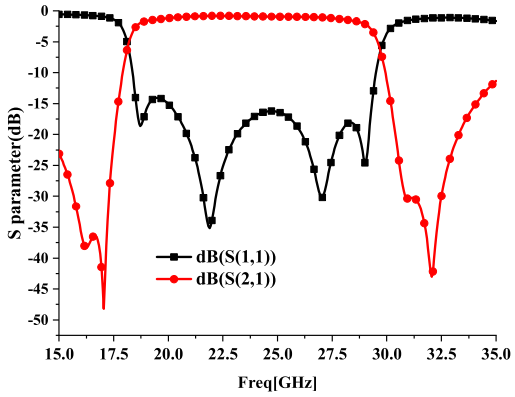

FIGURE 10. Frequency response simulation curve of square resonant loop filter loaded with open-circuit stubs.

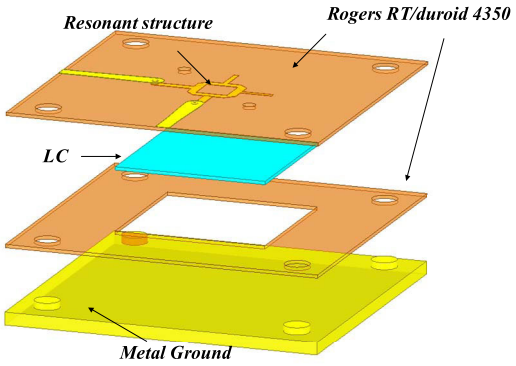

FIGURE 11. Filter structure.

located on the lower surface of the substrate and contacts with the middle liquid crystal to realize frequency adjustability. To ensure liquid crystal injection, a pair of through holes are processed in the upper liquid crystal substrate to inject liquid crystal. The middle liquid crystal layer uses 0.254mm thick substrate and mill out rectangular slots to accommodate the liquid crystal. The liquid crystal model used in this paper is AY71-007, which effective dielectric constant varies from 2.4 to 3.6 with the tangent loss angle being 0.01.

The designed filter structure is given in Fig. 11. To prevent the circuit from deforming, the whole circuit substrate uses Rogers 4350 substrate with high hardness. The frequency response and group delay are displayed in Fig. 12(c).

As there are no low frequency short circuit and open circuit in the whole filter structure, the liquid crystal bias voltage can be added through the RF port. In the test system shown in Fig. 14, we use the PNA-X vector network analyzer of Keysight Technologies, which has built-in Bias-T module and provides the bias loading port for the vector network. The function waveform signal generator provides 1KHz low frequency square wave signal modulation voltage (0V-20V), which is loaded onto the device under test through the radio frequency input port. Considering the influence of liquid crystal dielectric constant on the characteristic impedance, the final circuit size is determined by numerical optimization as follows: $L_1 = 3.4$mm, $L_2 = 2.5$mm, $L_3 = 2.45$mm, $W_1 = 0.2$mm.

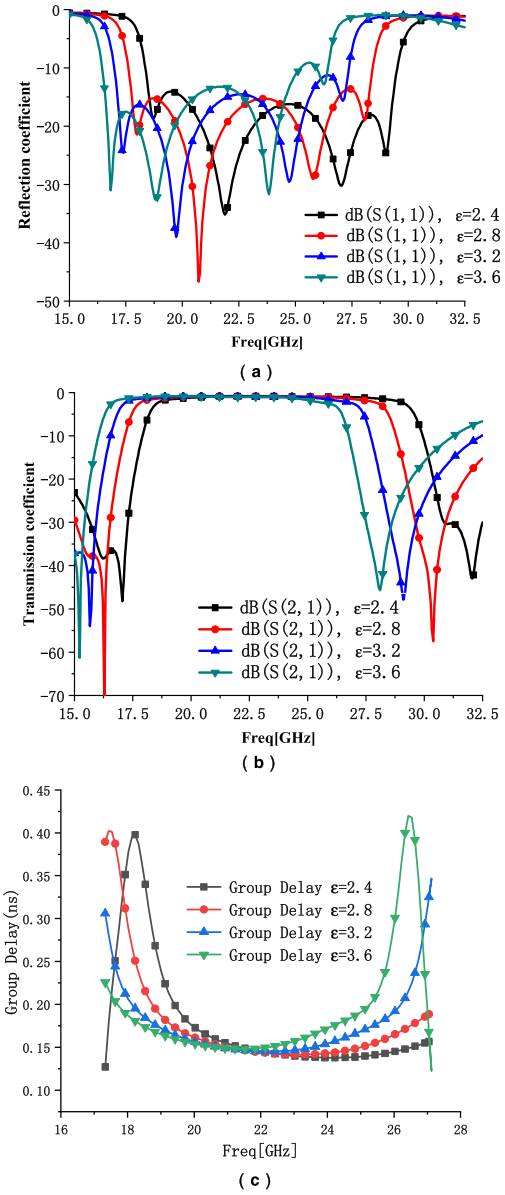

FIGURE 12. The filter simulation results (a) Return loss (b) Insertion loss (c) Group delay.

The part in contact with the liquid crystal layer is suspended by polyimide with parallel orientation, so the dielectric constant of the liquid crystal increases with the increase of bias voltage. The electric size of the filter increases with the increase of bias voltage, and the resonance frequency of the inverted center will move to low frequency.

From Fig.15, we can see that when the bias voltage is greater than 10V, the maximum tuning value of liquid crystal is reached, and the liquid crystal molecule perpendicular to the Poynting vector becomes parallel to the Poynting vector. Since bubbles are introduced in the process of liquid crystal injection and packaging, the Q value of the circuit is reduced, and the other two transmission zeros are invisible. The frequency response reconstruction range of the filter is 12%, the relative bandwidth before and after tuning is 48.17%

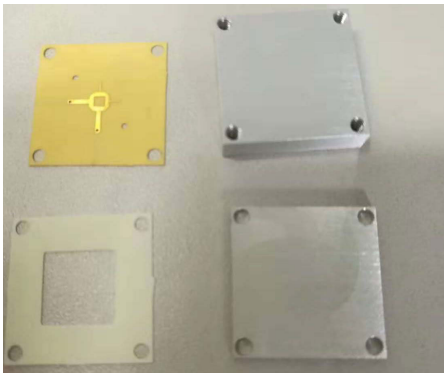

(a)

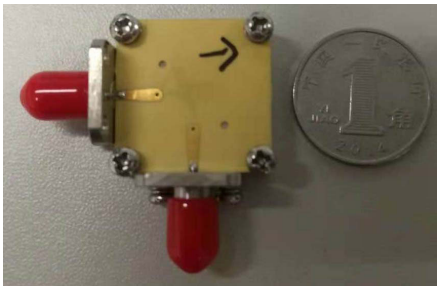

(b)

FIGURE 13. Physical diagram of filter (a) Pre-assembly (b) Post-assembly.

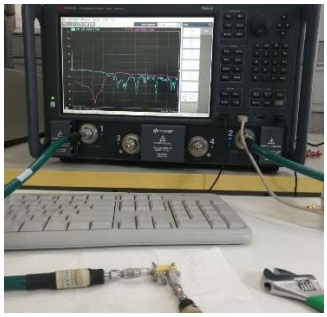

FIGURE 14. Filter test platform.

to 49.82%, respectively. The insertion loss in passband is less than 5dB. The frequency response is well preserved, which verifies the feasibility of realizing frequency reconstruction of liquid crystal in K and Ka bands. Fig.15(c) is the group delay result of the test. The in-band group delay is always less than 0.45ns before and after the filter reconstruction, indicating that the filter has good transmission characteristics.

Comparing the simulation results with the test results, we found that the tested return loss is worse than the simulation results due to the existence of bubbles in the liquid crystal layer, which make the liquid crystal distributed unevenly in the cavity and cause unnecessary influences.

Table 1 compares the parameters of our designed reconfigurable filters with the frequency reconfigurable filters in literature.

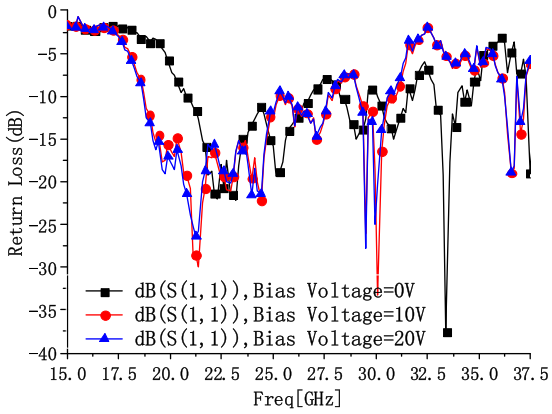

(a)

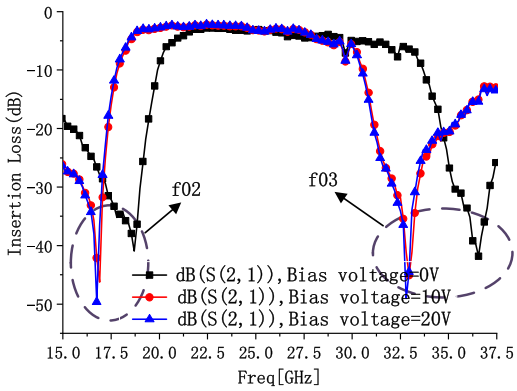

(b)

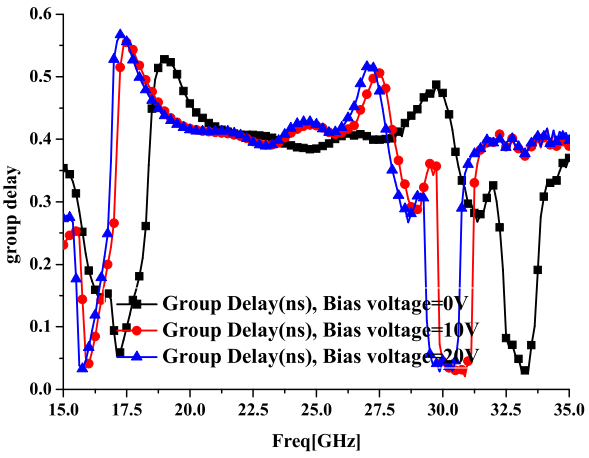

(c)

FIGURE 15. Test results (a) Return loss (b) Insertion loss (c)Group delay.

IV. CONCLUSION

In this paper, a wideband band-pass frequency tunable filter was designed with liquid crystal for K-band applications. Experimental results show that the reconfigurable central frequency varies from 27.7GHz to 24.6GHz, and the reconfigurable frequency range is 12%.

REFERENCES

[1] M. F. Karim, Y.-X. Guo, Z. N. Chen, and L. C. Ong, "Miniaturized reconfigurable and switchable filter from UWB to 2.4 GHz WLAN using PIN diodes," in *IEEE MTT-S Int. Microw. Symp. Dig.*, Boston, MA, USA, Jun. 2009, pp. 509–512.

[2] P. Vryonides, S. Nikolaou, S. Kim, and M. M. Tentzeris, "Reconfigurable dual-mode band-pass filter with switchable bandwidth using PIN diodes," *Int. J. Microw. Wireless Technol.*, vol. 7, no. 6, pp. 655–660, 2014.

[3] M. Ou, Y. He, and L. Sun, "A novel reconfigurable bandpass filter using varactor-tuned stepped-impedance-stubs," in *Proc. Int. Symp. Antennas Propag.*, Nanjing, China, Oct. 2013, pp. 754–756.

[4] H. A. Mohamed, H. B. El-Shaarawy, E. A. F. Abdallah, and H. M. El-Hennawy, "Frequency-reconfigurable microstrip filter with dual-mode resonators using RF PIN diodes and DGS," *Int. J. Microw. Wireless Technol.*, vol. 7, no. 6, pp. 661–669, 2015.

[5] H. Jiang, "Miniaturized and reconfigurable CPW square-ring slot antenna using thin film varactor technology," in *IEEE MTT-S Int. Microw. Symp. Dig.*, Baltimore, MD, USA, Jun. 2011, pp. 1–4.

[6] C. Yoon, S.-G. Hwang, G.-C. Lee, W.-S. Kim, H.-C. Lee, and H.-D. Park, "A reconfigurable antenna using varactor diode for LTE MIMO applications," *Microw. Opt. Technol. Lett.*, vol. 55, no. 5, pp. 1141–1145, 2013.

[7] M. N. M. Kehn, Ó. Quevedo-Teruel, and E. Rajo-Iglesias, "Reconfigurable loaded planar inverted-f antenna using varactor diodes," *IEEE Antennas Wireless Propag. Lett.*, vol. 10, pp. 466–468, 2011.

[8] Y. Yang, Y. Cai, K. Y. Chan, R. Ramer, and Y. J. Guo, "MEMS-loaded millimeter wave frequency reconfigurable quasi-Yagi dipole antenna," in *Proc. Asia–Pacific Microw. Conf.*, Melbourne, VIC, USA, Dec. 2011, pp. 1318–1321.

[9] C. W. Jung, M.-J. Lee, G. P. Li, and F. De Flaviis, "Reconfigurable scan-beam single-arm spiral antenna integrated with RF-MEMS switches," *IEEE Trans. Antennas Propag.*, vol. 54, no. 2, pp. 455–463, Feb. 2006.

[10] M. Unlu, Y. Damgaci, H. S. Mopidevi, O. Kaynar, and B. A. Cetiner, "Reconfigurable, tri-band RF MEMS PIFA antenna," in *Proc. IEEE Int. Symp. Antennas Propag. (APSURSI)*, Spokane, WA, USA, Jul. 2011, pp. 1563–1565.

[11] J.-Q. Zhu, Y.-L. Ban, C.-Y.-D. Sim, and G. Wu, "NFC antenna with nonuniform meandering line and partial coverage ferrite sheet for metal cover smartphone applications," *IEEE Trans. Antennas Propag.*, vol. 65, no. 6, pp. 2827–2835, Jun. 2017.

[12] W. Fuscaldo, P. Burghignoli, P. Baccarelli, and A. Galli, "Efficient 2-D leaky-wave antenna configurations based on graphene metasurfaces," in *Proc. 46th Eur. Microw. Conf. (EuMC)*, London, U.K., Oct. 2016, pp. 313–316.

[13] A. E. Prasetiadi, O. H. Karabey, C. Weickhmann, T. Franke, W. Hu, M. Jost, M. Nickel, and R. Jakoby, "Continuously tunable substrate integrated waveguide bandpass filter in liquid crystal technology with magnetic biasing," *Electron. Lett.*, vol. 51, no. 20, pp. 1584–1585, Oct. 2015.

[14] M. Roig, M. Maasch, C. Damm, and R. Jakoby, "Liquid crystal-based tunable CRLH-transmission line for leaky wave antenna applications at Ka-Band," *Int. J. Microw. Wireless Technol.*, vol. 6, nos. 3–4, pp. 325–330, 2014.

[15] D. Jiang, Y. Liu, X. Li, G. Wang, and Z. Zheng, "Tunable microwave bandpass filters with complementary split ring resonator and liquid crystal materials," *IEEE Access*, vol. 7, pp. 126265–126272, 2019.

[16] S. Sun and L. Zhu, "Wideband microstrip ring resonator bandpass filters under multiple resonances," *IEEE Trans. Microw. Theory Techn.*, vol. 55, no. 10, pp. 2176–2182, Oct. 2007.

[17] F. Goelden, A. Gaebler, O. Karabey, M. Goebel, A. Manabe, and R. Jakoby, "Tunable band-pass filter based on liquid crystal," in *German Microw. Conf. Dig. Papers*, Mar. 2010, pp. 98–101.

[18] M. Yazdanpanahi and D. Mirshekar-Syahkal, "Millimeter-wave liquid-crystal-based tunable bandpass filter," in *Proc. IEEE Radio Wireless Symp.*, Santa Clara, CA, USA, Jan. 2012, pp. 139–142.

[19] N. Vahabisani, S. Khan, and M. Daneshmand, "Microfluidically reconfigurable rectangular waveguide filter using liquid metal posts," *IEEE Microw. Wireless Compon. Lett.*, vol. 26, no. 10, pp. 801–803, Oct. 2016.

[20] T. Cheng and K.-W. Tam, "A wideband bandpass filter with reconfigurable bandwidth based on cross-shaped resonator," *IEEE Microw. Wireless Compon. Lett.*, vol. 27, no. 10, pp. 909–911, Oct. 2017.

[21] A. E. Prasetiadi, J. Matthias, B. Schulz, M. Quibeldey, T. Rabe, R. Follmann, and R. Jakoby, "Liquid-crystal-based amplitude tuner and tunable SIW filter fabricated in LTCC technology," *Int. J. Microw. Wireless Technol.*, vol. 10, nos. 5–6, pp. 674–681, 2018.

[22] E. Polat, R. Reese, M. Jost, C. Schuster, M. Nickel, R. Jakoby, and H. Maune, "Tunable liquid crystal filter in nonradiative dielectric waveguide technology at 60 GHz," *IEEE Microw. Wireless Compon. Lett.*, vol. 29, no. 1, pp. 44–46, Jan. 2019.

DI JIANG received the M.S. and Ph.D. degrees in electromagnetic field and microwave technology from the University of Electronic Science and Technology of China (UESTC), Chengdu, China. Since 2014, he has been an Associate Professor in electromagnetic fields and microwave techniques with the School of Information and Communication Engineering, University of Electronic Science and Technology of China. His research interests include high-performance microwave and millimeter-wave reconfigurable devices, antennas, and microwave device modeling. Especially, he has applied liquid crystal materials to the design of microwave and millimeter-wave devices.

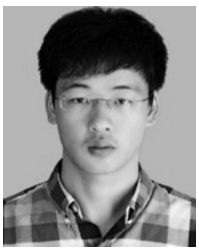

XIAOYU LI is currently pursuing the M.S. degree with the School of Information and Communication Engineering, University of Electronic Science and Technology of China, Chengdu, China. His research interests include liquid crystal technologies and reconfigurable antenna/array.

ZIHAO FU is currently pursuing the Ph.D. degrees with the School of Physics, University of Electronic Science and Technology of China, Chengdu, China. His current research interests mainly include the tunable RF and microwave passive circuits research, and pattern-reconfigurable antennas analysis and design.

GUOFU WANG was born in Pingdingshan, China, in 1977, and the M.S. and Ph.D. degrees in signal and information processing from the Chinese Academy of Sciences, in 2005 and 2007, respectively. Since 2017, he has been a Professor with the School of Electrical and Information Engineering, Guangxi University of Technology. His main research include adaptive signal processing and image processing, which have rich research experience in the development of key technologies of photoelectric countermeasure turntable.

ZHI ZHENG (M'11) received the M.S. and Ph.D. degrees in electronic engineering and information communication engineering from the University of Electronic Science and Technology of China (UESTC), Chengdu, China, in 2007 and 2011, respectively. From 2014 to 2015, he was an Academic Visitor with the Department of Electrical and Electronic Engineering, Imperial College London, U.K. Since 2011, he has been with the School of Information and Communication Engineering, UESTC, where he is currently an Associate Professor. His research interests include statistical and array signal processing, including direction finding, source localization, target tracking, sparse array design, robust adaptive beamforming, jammer suppression, compressive sensing, machine learning, and convex optimization, with applications to radar, sonar, satellite navigation, wireless communications, and wireless sensor networks.

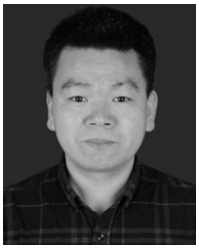

TIANLIANG ZHANG (M'12) was born in August 1976. He received the M.S. and Ph.D. degrees in physical electronics from the University of Electronic Science and Technology of China (UESTC), Chengdu, China, in 2004 and 2009, respectively. He is currently a full-time Professor with UESTC. His research interests include microwave theory and technology, and microwave and millimeter wave circuits and systems.

WEN-QIN WANG (M'08–SM'16) received the B.S. degree in electrical engineering from Shandong University, Shandong, China, in 2002, and the M.E. and Ph.D. degrees in information and communication engineering from the University of Electronic Science and Technology of China (UESTC), Chengdu, China, in 2005 and 2010, respectively. From 2005 to 2007, he was with the National Key Laboratory of Microwave Imaging Technology, Chinese Academy of Sciences, Beijing, China. From 2011 to 2012, he was a Visiting Scholar with the Stevens Institute of Technology, NJ, USA. From 2012 to 2013, he was a Hong Kong Scholar with the City University of Hong Kong, Hong Kong. From 2014 to 2016, he was a Marie Curie Fellow with Imperial College London, U.K. Since 2007, he has been with the School of Communication and Information Engineering, UESTC, where he is currently a Professor. He has authored two books published, respectively, by Springer and CRC Press. His research interests include array signal processing and its applications in radar, communications, and electronic warfare. He is the Editorial Board member of four international journals. He was a recipient of a Marie Curie International Incoming Fellowship, the National Young Top-Notch Talent of the Ten-Thousand Talent Program Award, and a Hong Kong Scholar Fellowship.